Practical experiences of battery operation in a Norwegian rural grid

Kine Strupstad[a], Jon Arnesen[b], Simen Karlsen[c], Håkon Duus[d], Hanna Sletta[e]

[a]*Peak Shaper, kine.ryberg@eidsiva.no,*
[b]*Tensio, jon.arnesen@tensio.no,*
[c]*Multiconsult, simen.karlsen@multiconsult.no,*
[d]*Multiconsult, hakon.duus@multiconsult.no,*
[e]*Multiconsult, hanna.sletta@multiconsult.no,*

Abstract

With increasing energy consumption and the rise of variable renewable energy sources seen today, new possibilities in the changing energy landscape have to be investigated. Battery technology used as energy storage is a promising concept that can be used to improve quality of supply and to avoid expensive grid expansions. In this paper, the impact of Battery Energy Storage Systems (BESS) on power grid operations is examined. To investigate this, a pilot case with a 1 MW / 1 MWh battery installed in the distribution system in Lierne, Trøndelag in Norway was put through six tests.

Findings show a strong degree of voltage stabilisation through managing active and reactive power feed-in from the battery. This is especially true for reactive power exchange, which shows multiple positive aspects across different applications, including reduced system losses and mitigation of adverse effects from rapid battery charging. The positive impacts of the battery system were additionally found to permeate well through the 22 kV system, with less than 15 % reduction in voltage strengthening capabilities within 6 km of the battery.

Throughout the performed tests, BESS is shown to be a powerful tool for grid strengthening and loss reduction in distribution networks. Based on the study's findings, battery systems show the potential to greatly improve quality of supply in weak grids and prolong the lifetime of distribution infrastructure. Additionally, this is shown to be achievable with negligible negative impacts from battery charging.

With the ability of independent actors such as Peak Shaper to provide services to ancillary markets while simultaneously tackling local system challenges, BESS demonstrates strong economic and technical viability in distribution system operations.

Keywords: Battery storage, voltage control, rural grids, grid services, battery as-a-service, frequency markets

1. Introduction

In Norwegian grid regulation law, there is a firm separation between grid operators and power producers to ensure fair trading in all markets, and to make sure that grid operators does not exploit their monopoly powers. A power grid operator is therefore not allowed to own any form of power production (1). To utilise batteries for selling power in an electricity market is therefore not permitted if power grid operators themselves own the batteries (2).

Peak Shaper is an advisory service delivered by the Norwegian company Eidsiva Vekst. Peak Shaper offers batteries as a leasing service to distribution system operators (DSO) and commercial actors. The ambition of Peak Shaper is to enable better use of the power system by reducing power transmission bottlenecks through the use of batteries. The bottlenecks can be both thermal overloads, or weak radials causing voltage drops. Additionally, the batteries can extend the lifetime of existing power infrastructure, creating large savings in capital cost for the DSOs.

This whitepaper will describe and discuss real measurements and results from a pilot case utilising Peak Shaper's battery installations. The installation used in the study is located in a weak rural distribution grid, and will demonstrate local voltage improvement, loss reduction, as well as participation in the national frequency markets.

1.1. Pilot description

The Lierne battery pilot resides in Trøndelag county, Norway, in a rural area close to the Swedish border. A map of the area with measurement points used in the tests is shown in Figure 1. The Nordli transformer station is connected to the 66 kV regional grid, and from here a 40 km long 22 kV overhead line feeds the Lierne area. The grid is operated by the regional distribution system operator, Tensio (3).

Connected to this line are multiple industrial consumers whose consumption is a significant portion of the nominal load in the area. These consumers have also expressed a desire to expand their operations, increasing local power demand. Such a load increase would demand capacity upgrades on the 22 kV line to keep voltages within statutory standards, and, according to Tensio, incur costs in the scale of tens of million NOK (several million EUR). This cost is disproportionately large compared to the size and revenue of this local industrial actors, and is not sustainable for them to take.

The proposed and current solution has been for Tensio to lease a 1 MW / 1 MWh battery from Peak Shaper, a Norwegian start-up company specialising in leasing battery services to DSOs and industrial clients. The setup with a leased battery to a DSO is the first of its kind in Norway, and one of very few large battery installations in rural grids.

The battery itself is placed in close physical proximity to the industrial costumer Liskifer, with a separate 400 V / 22 kV transformer feeding directly in to the medium voltage distribution grid.

An important part of the pilot project is to verify the actual benefit of the battery. How it affects the local grid, can enable increased loads, better voltage control, and reduce losses.

2. Methodology

2.1. Test setup

The tests were conducted in the period April to September 2023. Measurements were collected from the Nordli substation, through the battery control software of Pixii, from all local AMI meters, a sub-selection of AMI meters, and from a selection of advanced power meters in the area. A simple map of the area and placements of the power meters is given in Figure 1 with the 22 kV grid lines visible in green, and the sub-selection of AMI meters numbered 1-10. A corresponding simplified single line diagram (SLD) is given in Figure 2. The battery is placed by point 1 in the figure. The approximate electrical distance from the battery to the respective AMI meters is given in Table 1.

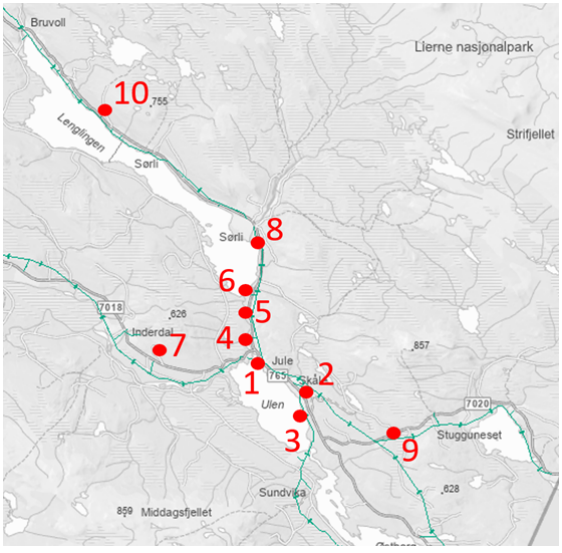

Figure 1: Map of distribution lines at Lierne with the measurement point locations (3)

To ensure a thorough assessment of the Lierne battery's capabilities and added value, six different tests were planned and conducted. The primary service of the battery in Lierne is to act as a grid-strengthening unit, and thus the test plan focuses on voltage services. Below is a list of the conducted tests, and a full account of the test setup for each.

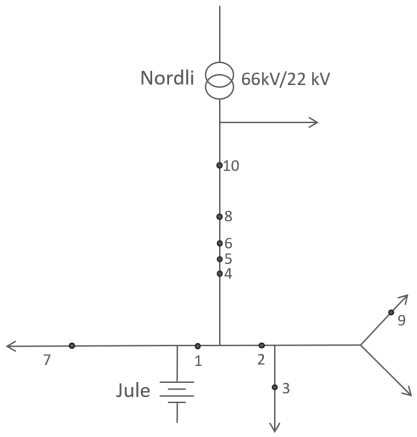

Figure 2: A single line diagram showing the power system in Lierne as well as the placement of the meters used for measurements in Test B

Table 1: Approximate electrical distance from the BESS of the sub-selection of AMI meters

Measurement point	Electrical distance from BESS (m)
Meter 1	20
Meter 2	1 000
Meter 3	1 500
Meter 4	2 000
Meter 5	3 000
Meter 6	4 200
Meter 7	5 000
Meter 8	6 000
Meter 9	7 000
Meter 10	14 000

1. Test A - Voltage support
2. Test B - Voltage propagation
3. Test C - Loss reduction
4. Test D - Passive voltage support
5. Test E - Fast Frequency Response (FFR) market qualification and participation
6. Test F - NETBAS grid model verification

2.2. Test A - Voltage support

Although the purpose of the battery system is to support the local grid in times of high demand and low voltage, it will need to recharge in order to serve its purpose through multiple cycles. The act of charging the battery can cause an increased strain on the grid if not performed with forethought. The negative effects can be mitigated in multiple ways, such as charging at low power draw, charging at times when the margin of voltage stability in the grid is large (often low-demand hours), and compensating with reactive power feed-in during charging cycles.

Test A - voltage support focus on assessing how the voltage in the grid is affected by charging and discharging the battery using different configurations of active and reactive power, or

a combination of the two. The tests were conducted on August 10^{th} 2023, which was a Thursday with a relatively normal consumption profile.

The charging or discharging sequence in each step was kept for 2 minutes, followed by a 2 minute rest period without the battery exchanging power. After the 2 minute rest period, which also served as control measurement, the next step in the test was initiated. The measuring frequency of the voltage during the full duration of *Test A* was 30 seconds. The measurements were taken with a SafeBase (elspec) meter, placed at the Jule circuit breaker, illustrated in the single line diagram in Figure 2.

The battery discharge (grid feed-in) sequence was conducted with three different cases, namely active, reactive and complex power feed-in. The power-factor (PF) for each case was PF=1.0, PF=0.2, and PF=0.707 respectively. Each case was tested in four different steps, with increasing apparent (total) power.

Table 2 displays the real active and reactive components for each case and each step, 12 in total.

Table 2: Amount for power discharged during Test A

Step	**Active power feed-in**	**Reactive power feed-in**	**Complex power feed-in**
1	0.25 MW + 0 MVAr	0.051 MW + 0.25 MVAr	0.177 MW + 0.177 MVAr
2	0.50 MW + 0 MVAr	0.102 MW + 0.50 MVAr	0.354 MW + 0.354 MVAr
3	0.75 MW + 0 MVAr	0.153 MW + 0.75 MVAr	0.530 MW + 0.530 MVAr
4	1.00 MW + 0 MVAr	0.205 MW + 1.00 MVAr	0.707 MW + 0.707 MVAr

Similarly, during the battery charging sequence, two different cases with active and reactive power were tested, with three and four different steps, respectively. Parameters for the charging tests are shown in Table 3.

Table 3: Amount for power charged during Test A

Step	**Active power charging**	**Active power charging w/reactive feed-in**
1	-0.25 MW + 0 MVAr	-0.75 MW + 0.375 MVAr
2	-0.50 MW + 0 MVAr	-1.00 MW + 0.500 MVAr
3	-0.75 MW + 0 MVAr	-1.00 MW + 0.250 MVAr
4	-1.00 MW + 0 MVAr	-

2.3. Test B - Voltage propagation

When installing batteries in the power system, they often target a relatively local issue. *Test B - Voltage propagation*, was set up to measure the effect the battery has on the low voltage distribution system in the wider area around the installation. The low voltage distribution grid in the area is a 230 V-IT grid, which is common in Norway, and the voltage should be within ±10% of the nominal (4).

The DSOs Advanced Metering Infrastructure (AMI) was used to collect voltage measurements from a selection of sites, shown in Figure 1, also listed in Table 1. The corresponding electrical distance is also shown, the furthest being 14 km away. During testing, meter 9 was not measured correctly, and data for this meter is not mentioned further in this paper. The term "electrical distance" refers to the distance the power travels along the power lines between the battery installation and the respective meter. The voltage was also measured at the Jule circuit breaker, in immediate proximity to the battery, as described in *Test A*.

The AMIs are providing voltage measurements on a 5 minute resolution, while the measurements at Jule were recorded every 30 seconds. Each test sequence was run for 5 minutes, followed by a 5 minute rest period with zero power exchange on the battery to provide a control measurement, before commencing on the next test.

Test 1, 2, and 3 were all discharging tests, where the battery was injecting active and reactive power to the grid, with the purpose of lifting the voltage. Test 4 was a charging test, performed to assess the effect on the grid voltage when the battery is charging at full power. The power composition for each test is given in Table 4.

Table 4: Amount for power discharged and charged during Test B

Test	Power composition
Test 1: Active power discharge	1.000 MW + 0 MVAr
Test 2: Reactive power PF = 0.38	0.410 MW + 1 MVAr
Test 3: Reactive power PF = 0.2	0.205 MW + 1 MVAr
Test 4: Active power charging	- 1.000 MW + 0 MVAr

Nordli transformer has an automatic tap changer. During test sequence 2 it was observed that Nordli transformer automatically tapped down to compensate for the raised voltage caused by the test sequence. The log from the transformer tap settings is presented in Figure 3, and indicates that the transformer taps down around 12:12 and back up at around 12:32 on August 10^{th}, during *Test B*.

This tap change affects the measured voltage at the AMIs used in the test, as well as the voltage measurements at the Jule circuit breaker. To account for the tap-change and have comparable data before and after the tap change, the following methodology was adopted:

- Use of the 30 second voltage measurements from Jule to determine when in the test the tap change occurred
- Comparison of the control period before and after the tap change to determine the effect of the tap change on local voltage at the AMIs
- Weighting the AMI measurements during the tests according to the determined voltage change on the control periods

2.4. Test C - Loss reduction

By utilising the battery installation to feed reactive power into the grid, a portion of the reactive power required to magnetise the transmission infrastructure is provided locally as opposed to from the feeding transformer at Nordli substation. This can be leveraged to reduce current flow in the supplying line, which in turn may reduce both the voltage drop and system losses.

Test C - Loss reduction aimed to create such a loss reducing effect by feeding reactive power in at the battery site. The test was performed on September 11^{th}, from 09:00 to 23:00. To thoroughly assess the impact on system losses, the battery was

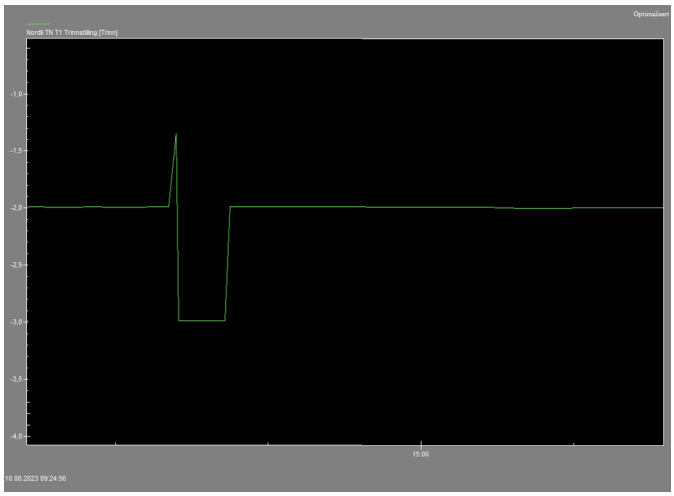

Figure 3: Log of tap-settings on Nordli transformer during Test B. The transformer briefly taps up and then down at 12:12 and back up at 12:32

injecting 486 kVAr reactive power for the complete duration of the test.

The power flow in the grid was measured at two instances, first of which was at the Nordli substation, measuring all active power flowing into the Lierne grid. At the other end, data was collected from all the AMIs in the area, thus measuring all the energy being *consumed* within the same section of the energy system. Both metering series had a measurement frequency of 1 hour. The difference between these two metering series constitutes the transmission losses in the grid for the given time step.

Baseline measurements of system losses from one week prior to the test, also collected using the method described above, were used as control measurements for evaluating the changes in losses from similar system states. To achieve control conditions similar to the test conditions, only the baseline measurements from the same time period from Monday to Thursday the week prior where used.

2.5. Test D - passive voltage support

In *Test A - Voltage support*, the battery's capacity to increase power through *active power* injection was measured. A downside of such voltage support, is that the battery inevitably must be charged at a later time, and consequently lower the voltage in the grid.

Test D - passive voltage support, seeks to quantify the voltage support from the battery by predominantly injecting reactive power to the grid, with only a minor active power component. This will drastically reduce the required charging of the battery, and also enable voltage support over longer time-periods.

The battery at Lierne is in reality two batteries of 500 kW / 500 kWh, which can be operated independently, and this is an advantage when conducting this test. The power electronics in the batteries cannot solely consume or produce reactive power, there must also be an active power component such that the power factor of the exchanged power stays above 0.2. To compensate for the active power requirement, voltage support was provided by discharging *battery A* with 356 kVAR reactive power, and charging it with 168 kW active power. Simultaneously, *battery B* would be discharging 150 kW active power. The net power exchange as seen from the grid would be a charging of the battery by 18 kW and a discharge of 356 kVAR. When *battery B* reached a State of Charge (SoC) of 30%, the battery states were switched such that *battery B* would be charging with active power and discharging reactive power, while *battery A would discharge active power*. This state would go on until *battery B* reached an upper SoC of 70%, at which point the states would be switched again.

The charge/discharge sequence for each battery is shown in Table 5, and illustrated in Figure 4.

Table 5: The charging and discharging states for the batteries at a given time during *Test D*. When the batteries reached a lower SoC of 30% or and upper SoC of 70%, the states would be switched

State	Battery A	Battery B
1	168 kW -356 kVAR	-150 kW + 0 kVAR
2	-150 kW + 0 kVAR	168 kW -356 kVAR

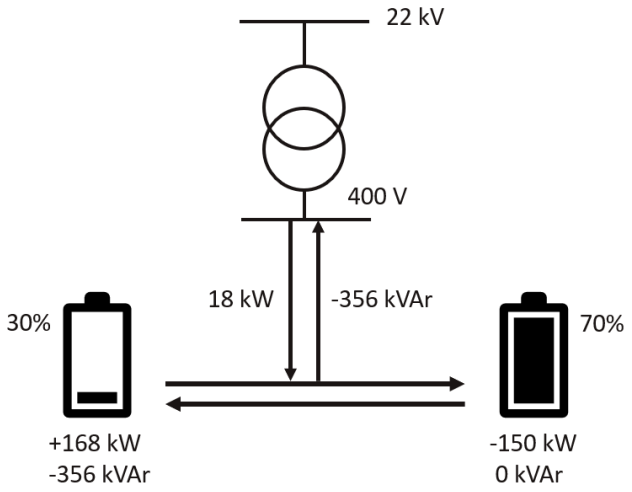

Figure 4: The transmission of power in the batteries during Test D

The resulting voltage measurements from this test were taken close to the Jule circuit breaker. To create a baseline for the effects of passive voltage support, the same meter was used to collect the voltage 28 days prior to the test, as well as 5 days after the test.

2.6. Test E - Fast Frequency Response (FFR) Qualification and participation

To ensure a steady frequency in the Nordic synchronous area, the Transmission System Operators (TSOs) of Norway, Sweden, and Finland purchase frequency reserves. These frequency reserves are currently bought nationally in a market, regulated by each TSO (5). To participate in the market, an asset must be pre-qualified for participation in the given market. Currently, the market in Norway which is most attractive for batteries

to participate in is the Fast Frequency Reserve (FFR) market, which requires a response time from the asset of less than 700 ms from a registered frequency event where the system frequency falls below 49.5 Hz. After activation, the asset is required to provide frequency support for a minimum of 30 seconds, and has to be ready for reactivation within 15 minutes (6).

The battery in Lierne is participating in the frequency market for the season of 2023. Prior to participation, the battery was pre-qualified. The pre-qualification process consists of testing the response time of the battery after a registered frequency event. In practice this entails setting the threshold for activation to a frequency very close to 50 Hz. In Lierne, the threshold was set to 49.999 Hz, with the battery participating with a total of 1.14 MW of frequency reserves.

2.7. Test F - NETBAS grid model verification

As an addition to the real-life tests, a replica of *Test A - Voltage support* was simulated in Tensio's Network Information System, NETBAS. The NETBAS Analysis module was used for the test, with a basis in the default grid model generated by NETBAS. Parameters for load and voltage were tuned to match our measured values on the day of real-life testing. To replicate the battery system, a Generator (GE) object was used in NETBAS, which can generate both active and reactive power in both directions of flow. The grid model in NETBAS is a comprehensive copy of the actual distribution grid in Lierne, without modelling simplifications, which means that simulated results should be similar to the real-life measurements. The main goal of this test is to verify whether the measured voltage variations from the different tests correspond with the results from the simulations, and further give an indication of the accuracy of the load-flow analysis in NETBAS for the purposes of simulating battery systems as voltage support in distribution grids.

The voltage increase simulated in NETBAS was then compared to the results found in *Test A - Voltage support*.

3. Results

In the following, the results from each test will be presented and discussed.

3.1. Results from Test A - Voltage support

The purpose of this test was to assess how the local voltage at Jule was affected by different patterns of charging and discharging power, investigating both active and reactive components.

The results are presented in the following order, active power feed-in (PF=1), reactive power feed-in (PF=0.2), and complex power feed-in (PF=0.707), followed by active power charging and charging with reactive feed-in. Power flow values for each case is given in Table 2 and Table 3.

Figure 5 depicts the voltage increase in each phase of the 22 kV grid at Jule with application of active power feed-in. The largest impact of active power feed-in is found at 0.25 MW and 0.5 MW, each step additively increasing the local voltage by about 200 V. The subsequent steps of 0.75 MW and 1 MW feed-in produce smaller voltage corrections, with the last step securing a proportionally low effect on the local voltage. Understanding this saturation dynamic, and at what stage the active power feed-in yields diminishing results, will be a key aspect for the grid operator, and may differ for varying operating states.

The next test sequence investigated voltage support through reactive power feed-in, with findings depicted in Figure 6. The results show a larger voltage increase per step, and a lower tendency of diminishing returns at higher values of feed-in compared to active power feed-in.

The last feed-in test in *Test A - voltage support*, was with a complex power feed-in, with a PF=0.707, depicted in Figure 7. This combination of active and reactive power feed-in results in the largest increase in grid voltage of the three battery discharge test sets. Again, the greatest voltage increase rate is observed at lower power levels, going from 0 to 0.25 apparent power, and 0.25 to 0.50 apparent power. The tendency of diminishing returns is also less evident for complex power feed-in, than for active power feed-in.

At the highest levels of complex power feed-in, the local voltage increased by 955 V, representing around 4.3% of the nominal voltage.

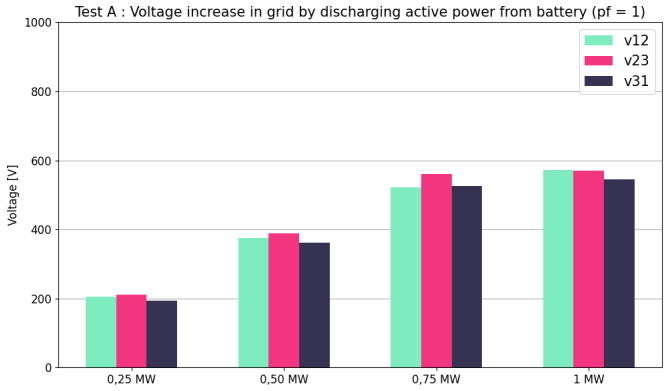

Figure 5: The voltage increase at Jule circuit breaker when discharge of active power (PF=1) from battery. Four different amounts of power feed-in are tested

In addition to investigating power feeding into the grid affects local voltage levels, power flow in the opposite direction was tested by monitoring local voltage while charging the battery. The first charging test was executed with active power, increasing charging in increments of 0.25 MW per step. The resulting effect on the local voltage is depicted in Figure 8, showing a clear trend of decreasing voltage as the battery charging power is increased.

As demonstrated in the previous test, and depicted in Figure 8, discharging reactive power from the battery will raise the grid voltage, and by extension, this can be used to compensate for active power consumption from the battery. This is demonstrated in the last test set of *Test A*, where the battery is charging active power, while simultaneously feeding reactive power to the grid. The voltage drop with reactive power compensation is presented in Figure 8. Investigating and comparing the

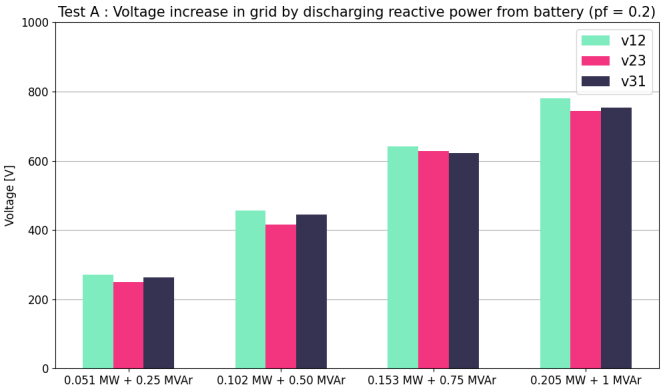

Figure 6: The voltage increase at Jule circuit breaker when discharge of reactive power (PF=0.2) from battery. Four different amounts of power feed-in are tested

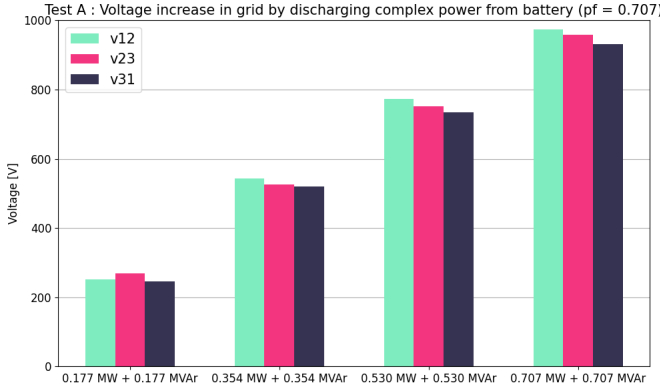

Figure 7: The voltage increase at Jule circuit breaker when discharge of complex power (PF=0.707) from battery. Four different amounts of power feed-in are tested

measurements to those made when charging with active power alone, it is evident that a significant portion of the voltage drop is mitigated through reactive compensation. A feed-in of 0.375 MVAr while charging 0.75 MW will reduce the local voltage loss of about 250 V in the 22 kV grid. Similarly, a 0.5 MVAr feed-in at 1 MW active power charging yields a voltage drop of around 400 V, compared to more than 800 V voltage drop without the reactive power component.

3.2. Test B - Voltage propagation

During *Test B - Voltage propagation* the battery was tested in five minute increments at four different discharge/charge configurations presented in Table 4. The three cases of battery power feed-in tested were active power (PF=1), complex power (PF=0.38), and reactive power (PF=0.2). The last case investigated charging the battery using active power. The timeline of the voltage during the different tests and control periods is shown in Figure 10. Here, the measured voltage has been corrected based on the tap changes mentioned in Section 2.3. The purpose of this test is to investigate how the battery activity spreads throughout the low voltage distribution grid.

The change voltage measured at Jule circuit breaker during the test cases is shown as a bar plot in Figure 11.

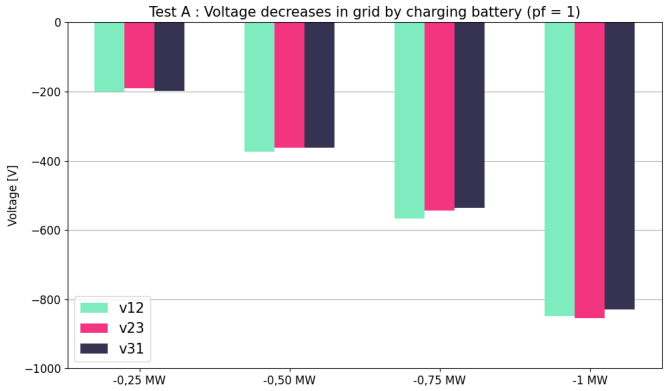

Figure 8: The voltage decrease at Jule circuit breaker when charging of active power (PF=1) to battery. Four different amounts of power are tested

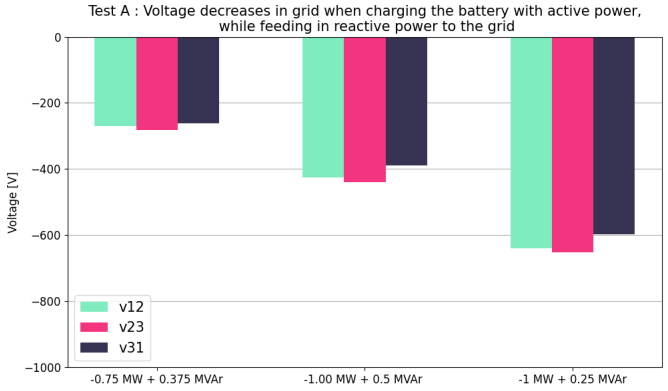

Figure 9: The voltage decrease at Jule circuit breaker when charging the battery with active power while feeding in reactive power at three different increments

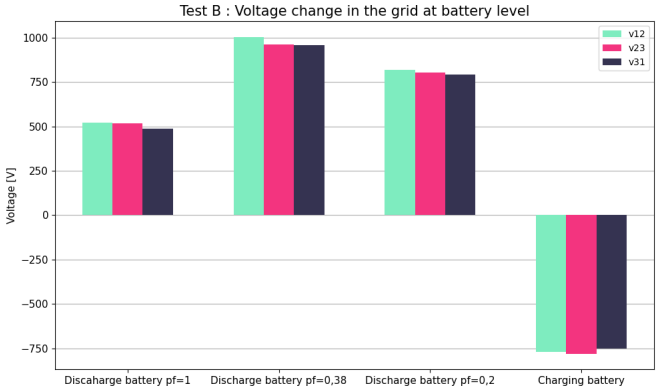

Figure 11: Voltage difference at Jule circuit breaker during Test B

In Figure 12, the increase in voltage during complex power discharge is shown as a contour plot, with AMI meter positions placed according to geographical coordinates. This shown propagation of the positive voltage increase in relation the the geographical placement.

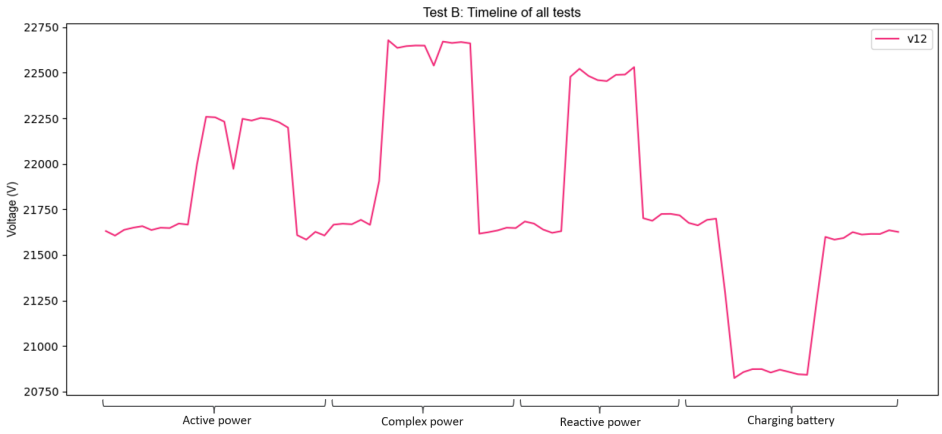

Figure 10: Longer time-series showing the real measured voltage during Test B. The three periods where the battery is discharging is clearly seen, followed by the period of charging the battery. The periods in between are control periods without battery activity

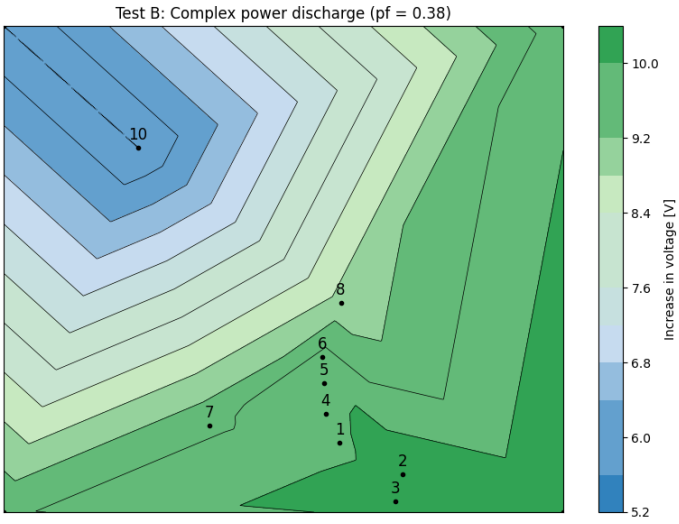

Figure 12: The voltage increase at nine AMI meters during complex power discharge in Test B

The change in voltage during battery activation at nine local consumers are shown as scatter plots in Figure 13, 14, 15, and 16. The nominal voltage at these metering points is 230 V. Here, the increase in voltage is plotted against the electrical distance between the AMI meters and the battery installation, also shown in Table 1. As expected, the general trend among the measurements shows reduced changes in voltage with increased electrical distance from the battery installation. As can be seen from Figure 15 and 16, meter 7 deviates from the trend in case 2 an 4. The map over Lierne in Figure 1 shown that meter 7 is connected to a branch without any of the other measurement points. Different conditions along this branch, such as fluctuations in downstream consumption and differing transmission hardware, is likely the cause of the deviation. The voltage at meter 1 also slightly differs from the trend seen among the remaining measurement points, showing somewhat smaller changes in voltage compared to slightly more distant meters. This meter is installed at the site of a large load, and is likely affected by this.

The first test case conducted was feed-in of active power from the battery to the grid. The result for the increase in voltage at the AMI meters is depicted in Figure 13. The largest increase in voltage was observed to be 5.4 V in meter 2, while the smallest is 2.65 V at meter 10.

Between the different test sets, feed-in of complex power, depicted in Figure 14, yields the highest voltage increase among meters within close proximity of the battery. Voltage increased in the range of 9.5 to 10.5 V among meters within 5 km of the battery system, an increase of 4.1% to 4.6% of nominal voltage. The voltage increase at meter 10, however, saw slightly better results during the feed-in of reactive power, at 6.5 V (2.8% of nominal).

As illustrated in Figure 10, charging the battery produces a local voltage drop comparable to the ones seen during *Test A*. The propagation of the voltage drop among the AMI meters is shown in Figure 16. As expected, metering points close to the battery see a larger drop than ones at larger distances. The spread in goes from approximately -6.8 V to -4.5 V, a respective change of 3% and 2% of the nominal voltage.

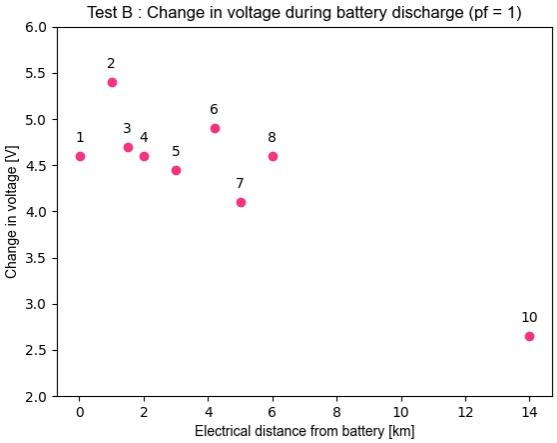

Figure 13: The voltage increase at nine AMI meters during battery discharge (PF=1) in Test B

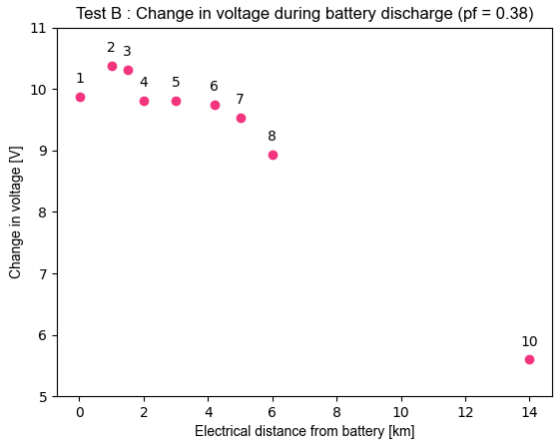

Figure 14: The voltage increase at nine AMI meters during battery discharge (PF=0.38) in Test B

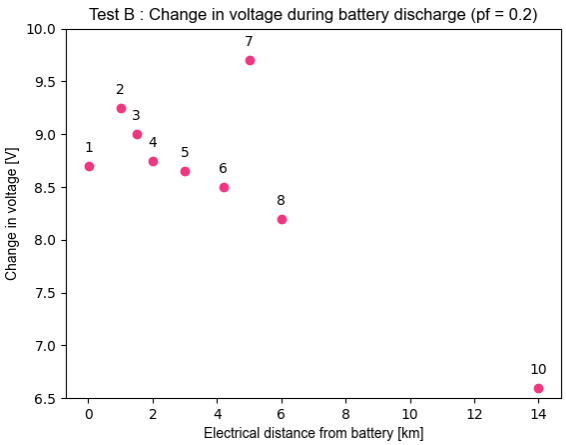

Figure 15: The voltage increase at nine AMI meters during battery discharge (PF=0.2) in Test B

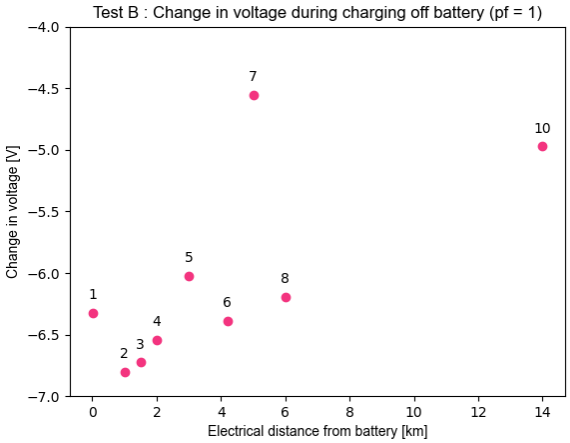

Figure 16: The voltage increase at nine AMI meters during battery charging in Test B

3.3. Test C - Loss reduction

Figure 17 shows system losses in the Lierne grid with and without the battery feeding reactive power into the grid. Compared to the control measurements, the losses are reduced by an average of 38.1 kWh/h, from 167.8 kWh/h to 129.7 kWh/h. This is a 22.7 % reduction of active power losses on the line.

Seen as a percentage of the load supplied, the losses are 8.44 % and 6.54 % without and with battery feed-in, respectively.

During the tests, it became evident that segments of the Lierne power system is ground cable based. This affects the reactive power balance of the distribution system, skewing it in a capacitive direction. It is likely that a similar system consisting entirely of overhead lines would see a larger reduction in losses due to a more inductive reactive power balance.

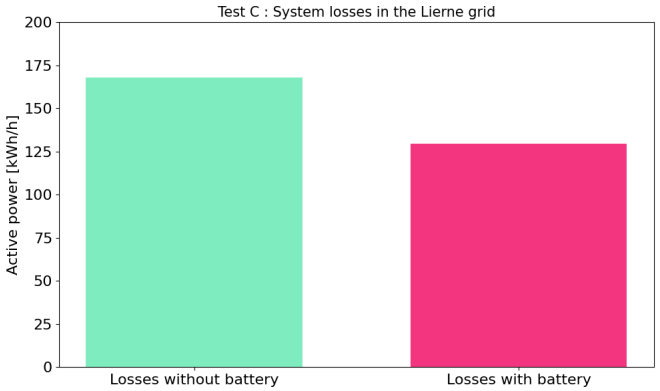

Figure 17: The system losses in the Lierne grid with and without battery support during Test C

3.4. Test D - Passive voltage support

The increase in voltage during passive voltage support from *battery A* and *B* in *Test D* is shown in Figure 18. One can observe that the average voltage increase in the distribution grid is around 400 V across all phases in the 22 kV grid. The batteries

were operated in accordance to the method outlined in Section 2.5, which was run continuously without the need to stop the reactive power feed-in to recharge the battery system.

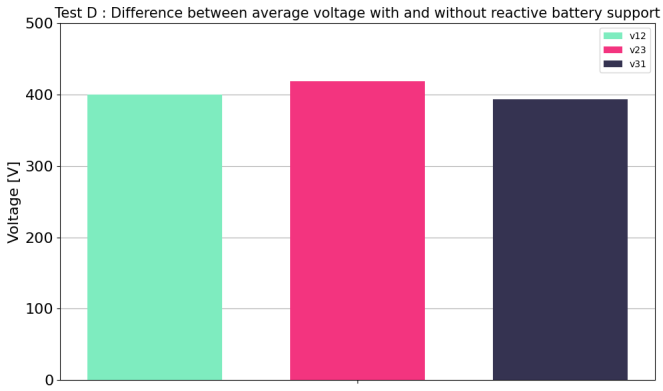

Figure 18: The increase in voltage during passive voltage support by the battery in Test D

3.5. *Test E- Fast Frequency Response (FFR) market qualification and participation*

Test E was conducted on both *battery A* and *B* and the response time to full production was found to be 0.579 s and 0.560 s, respectively. This is well within Statnett's response requirement of 0.7 s. The frequency curve and *battery A's* activation is shown in Figure 19, where the battery produced at its full capacity by the end of the response time. As demonstrated in the figure, the frequency falls below the requirement of 49.999 Hz at the start of the test, at t=0. At t=0.579 s, the battery system has reached the target power feed-in. The batteries where subsequently left to discharge for 42 s, well above the minimum requirement of 30 s.

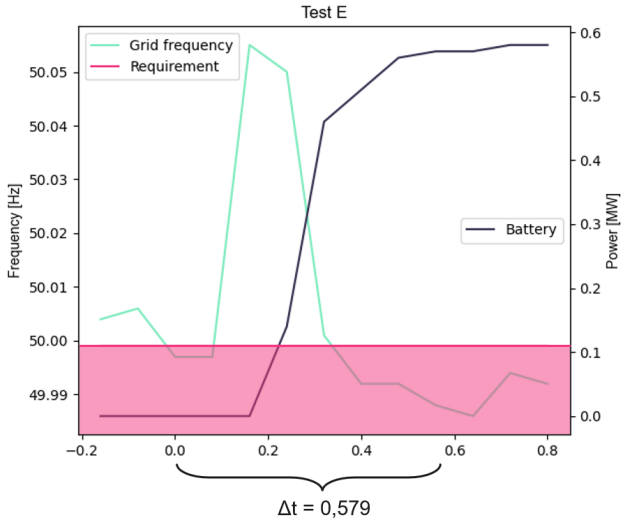

Figure 19: The frequency in the power grid and the production of *battery A* during Test E

3.6. *Test F - NETBAS grid model verification*

Test F aimed to compare measured results from real-life testing with results from simulations on the NETBAS grid model. As shown in Figures 20, 21, 22, 23, and 24, the measured change in voltage at the Jule circuit breaker was closely related to the results from NETBAS simulation. In most of the tests the measured voltage increase is larger than the NETBAS solution, the difference generally becoming larger at more total power charged/discharged. Even a higher power amounts, the difference in voltage increase is still not significant.

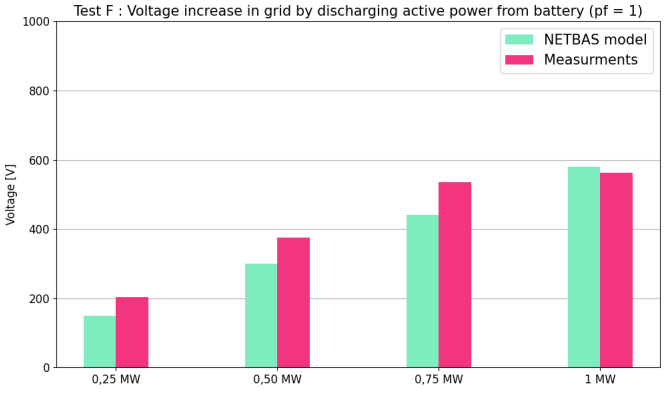

Figure 20: A comparison of voltage increase measured at Jule circuit breaker when feeding in active power (PF=1) from the battery, compared to the calculated increase in Netbas. Four different amounts of power are tested

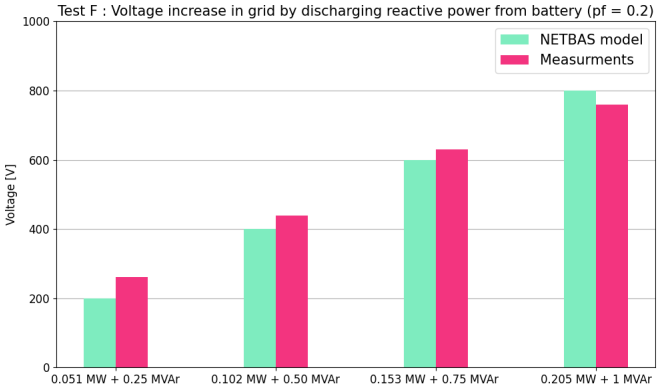

Figure 21: A comparison of voltage increase measured at Jule circuit breaker when feeding in reactive power (PF=0.2) from the battery, compared to the calculated increase in Netbas. Four different amounts of power are tested

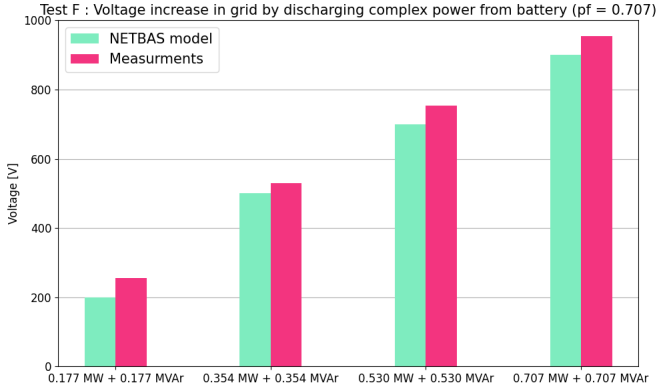

Figure 22: A comparison of voltage increase measured at Jule circuit breaker when feeding in complex power (PF=0.707) from the battery, compared to the calculated increase in Netbas. Four different amounts of power are tested

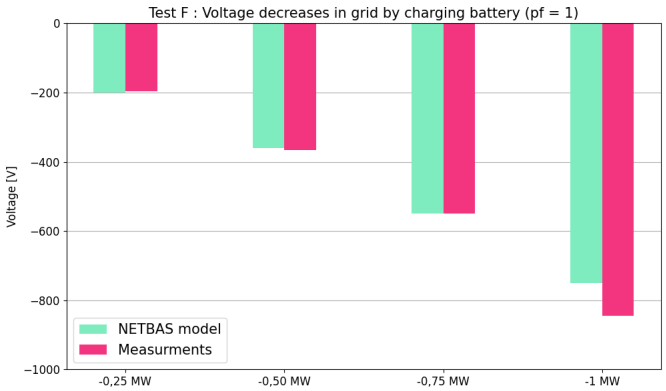

Figure 23: A comparison of measured and calculated voltage decrease at Jule circuit breaker when charging the battery with active power. Four different amounts of power are tested

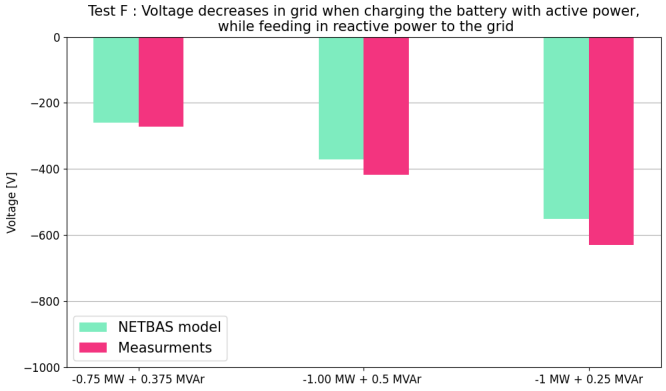

Figure 24: A comparison of measured and calculated voltage decrease at Jule circuit breaker when charging the battery with active power and feeding in reactive power to the grid. Three different amounts of power are tested

4. Discussion and conclusions

In both *Test A - Voltage support* and *Test B - Voltage propagation*, the largest increase in voltage occurs when the battery discharges complex power. The average local voltage increase during the feed-in of complex power amounts to 955 V, more than 4.3 % of the nominal voltage on the 22 kV line. In the low voltage grid, this yielded an increase of 9.5 V (4.1 %) within 5 km of the battery and 6.5 V (2.8 %) at meters 14 km away. The tests investigating feed-in of active and reactive power individually found significant although smaller yields in voltage stabilisation. This suggest a considerable voltage stabilising effect, which also propagates well throughout the grid, with considerable improvements at all investigated AMI meter locations.

The charging patterns investigated as part of *Test A - Voltage support* indicate that the adverse effects of high-power battery charging on the voltage can be significantly curtailed by simultaneous feeding reactive power back into the grid. As illustrated in Figure 8 and 9, the voltage drop from 1 MW of charging was halved from around 800 V to 400 V by applying 0.5 MVAr feed-in. This is a substantial improvement, providing options for battery operation with minimal effects on the surrounding grid. It is additionally worth noting that the battery charging can be conducted at a slower pace than in this test, something that would further reduce any voltage drop.

Test C - Loss reduction confirmed that continuous reactive feed-in from the BESS can reduce active power losses in the distribution grid. For the Lierne 22 kV line, this amounted to an average of 22.7 % reduction in losses. When applied over longer periods of time, such reductions in system losses can produce a sizeable economic benefit for the system operator. The prevalence of ground cables in the Lierne distribution grid may indicate that the potential of loss reduction could be even greater in a system entirely based on overhead lines.

The results presented in *Test D - Passive voltage support* showed that an increase of 400 V was achieved in the 22 kV grid through the use of reactive power feed-in, an improvement of 1.8 % of nominal voltage.

The operational patterns utilised during both *Test C - Loss reduction* and *Test D - Passive voltage support* are configured to be able to run indefinitely, without the need to stop and recharge the battery. This means that the benefits of both tests can be gained as a secondary advantage in addition to other battery operational purposes. This provides the system operator with powerful tools for grid strengthening and loss reduction.

A key takeaway from tests A, B, C, and D is that reactive power compensation will play a key role in battery operations in weak grids, and that the power electronics must be properly sized and specified to provide sufficient reactive power compensation for the desired application.

Additionally, this highlights the importance of understanding the local grid's response to active and reactive power injection when operating the battery on a day-to-day basis.

Test E - Fast Frequency Response (FFR) market qualification succeeded in qualifying the batteries provided by Peak Shaper for Statnett's Fast Frequency Response market in Norway. This shows the system-wide benefits and economical potential of batteries deployed in the distribution system. Although a power system operator may not own batteries for the purpose of acting on energy markets, independent actors such as Peak Shaper has the ability to provide services to ancillary markets and si-

multaneously solve challenges in the local distribution. This value stacking possibility could greatly improve the economic viability of BESS in distribution system operations.

Test F - NETBAS grid model verification shows that load-flow analysis performed in power system analysis software such as NETBAS produce results closely resembling physical measurements. Correspondingly, load-flow simulations can reliably predict the impacts a battery system will have on the power grid in steady state. This indicates that as long as the input to the grid model (e.g. line models, loads, and voltage) is adjusted properly, load-flow analysis may reliably be used in grid planning with BESS.

Acknowledgements

Thanks to Tensio for the opportunity to perform the BESS test, and for lending their direct assistance and deep understanding of power system operations to the project. Their insight has been invaluable to the results of the study and their contribution paramount to its completion.

Thanks to Pixii, supplier of the Lierne battery system, for eminent support in the testing stage, and detailed explanations to fully understand the capabilities of the battery installation. Without their devotion to this project, eye for quality in their product, and deep understanding of power electronics, this would not have been possible.

Appendix A. Time series measurements of Test A

Figure A.25 and A.26 shows the complete time series measurements of *Test A - Voltage support*, including both active testing periods and interspersed control periods.

References

[1] Standing Committee on Energy and the Environment. Innstilling fra energi- og miljøkomiteen om Endringer i energiloven m.m. (endringer om funksjonelt skille for nettforetak); 2021. Accessed 04.09.2023. [Online]. Available from: https://www.stortinget.no/no/Saker-og-publikasjoner/Publikasjoner/Innstillinger/Stortinget/2020-2021/inns-202021-183l/?all=true.

[2] NVE. Batteri tilknyttet nettet; 2023. Available from: https://www.nve.no/reguleringsmyndigheten/kunde/nett/tilknytning-av-forbruk-og-produksjon/batteri-tilknyttet-nettet/.

[3] NVE. NVE atlas; 2023. Available from: https://atlas.nve.no/Html5Viewer/index.html?viewer=nveatlas#.

[4] Ministry of Petroleum and Energy. Forskrift om leveringskvalitet i kraftsystemet; 2023. Available from: https://lovdata.no/dokument/SF/forskrift/2004-11-30-1557.

[5] Statnett. Raske frekvensmarkeder -FFR; 2023. Accessed: 2023-09-05. [Online]. Available from: https://www.statnett.no/for-aktorer-i-kraftbransjen/systemansvaret/kraftmarkedet/reservemarkeder/ffr/.

[6] Statnett. Vilkår for tilbud, aksept, rapportering og avregning i markedet for raske effektreserver (FFR); 2023. Accessed: 2023-09-12. [Online]. Available from: https://www.statnett.no/globalassets/for-aktorer-i-kraftsystemet/systemansvaret/retningslinjer-fos/systemansvaret---vedlegg-til-retningslinjer-for-fos--9---vilkar-for-ffr.pdf .

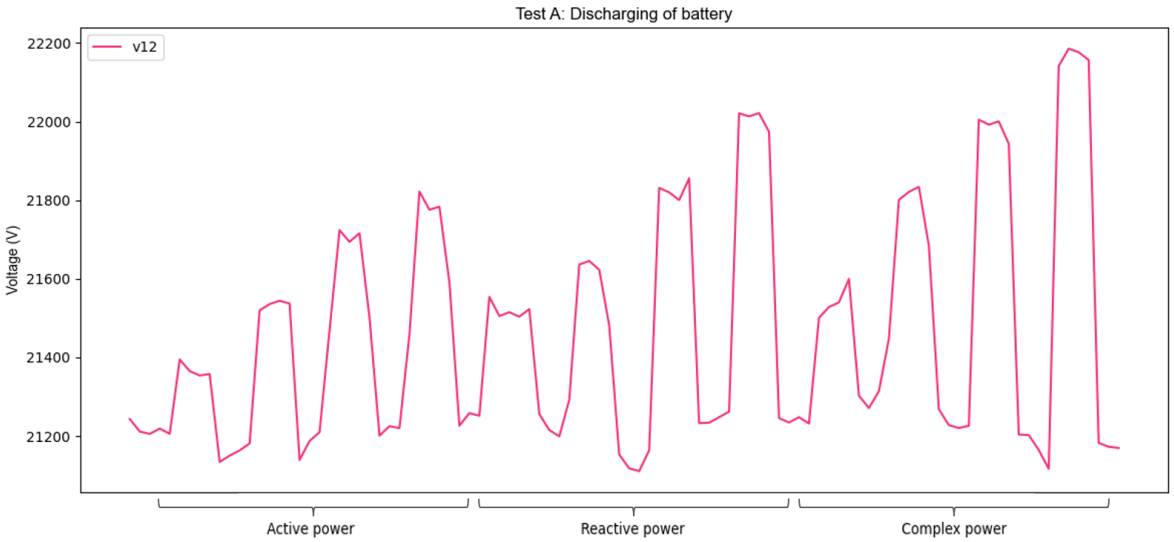

Figure A.25: Longer time series showing the real measured voltage during *Test A - Voltage support*'s discharging test sets. The periods where the battery is discharging are clearly seen as increases in voltage, followed by the rest-periods where voltage returns to normal levels

Figure A.26: Longer time-series showing the real measured voltage during *Test A - Voltage support*'s charging test sets. The periods where the battery is charging are clearly seen as drops in voltage, followed by the rest-periods where voltage returns to normal levels